Available online at www.sciencedirect.com

jmr&t
Journal of Materials Research and Technology

journal homepage: www.elsevier.com/locate/jmrt

Optimum operating parameters for PES nanocomposite membranes for mebeverine hydrochloride removal

Dhiyaa A. Hussein Al-Timimi [a], *Qusay F. Alsalhy* [a,*], *Adnan A. AbdulRazak* [a], *Mohammed Ahmed Shehab* [b,c], *Zoltán Németh* [d], *Klara Hernadi* [e]

[a] *Membrane Technology Research Unit, Chemical Engineering Department, University of Technology-Iraq, Alsinaa Street 52, 10066 Baghdad, Iraq*
[b] *Faculty of Materials and Chemical Engineering, University of Miskolc, H-3515 Miskolc, Hungary*
[c] *Polymers and Petrochemicals Engineering Department, Basrah University for Oil and Gas, Basrah 61004, Iraq*
[d] *Advanced Materials and Intelligent Technologies Higher Education and Industrial Cooperation Centre, University of Miskolc, H-3515 Miskolc, Hungary*
[e] *Institute of Physical Metallurgy, Metal Forming and Nanotechnology, University of Miskolc, H-3515 Miskolc-Egyetemváros, Hungary*

ARTICLE INFO

Article history:
Received 20 March 2023
Accepted 27 April 2023
Available online 2 May 2023

Keywords:
Nanocomposite membrane
Modified nanoparticles
Polyethylenimine
Pharmaceuticals
Wastewater treatment
Mixed matrix membrane
Optimization
Minitab 18

ABSTRACT

This study aims to optimize operating parameters of the effect of embedded silica nanoparticles (SiO_2 NPs) and modified silica NPs with polyethylenimine (PEI) (SiO_2-*g*-PEI NPs) into polyethersulfone (PES) to fabricate a mixed matrix membranes (MMMs) for pharmaceutical wastewater treatment. The performance of modified MMMs was compared in the separation of Mebeverine hydrochloride (MBV) from aqueous pharmaceutical wastewater. In order to produce a particular quantity of flux and rejection above desired levels, an optimization technique was used to find the best values for various important process parameters. To enhance the effectiveness on a bigger scale, response surface methodology (RSM) and analysis of variance (ANOVA) were utilized as mathematical and statistical approaches. This study examined the effects of operational parameters on the PES-NPs membranes permeate flux and MBV rejection for each sample. These parameters included SiO_2/or SiO_2-g-PEI NPs content (0.7–1 wt %), solution feed pH values (4-10), and MBV concentration (10–100 ppm). A mathematical model to calculate the permeate flux and rejection (%) was established. The results showed that the SiO_2 MMMs had the best performance of 38.27 LMH permeate flux and 81.26% of MBV rejection, while the permeate flux and MBV rejection % for SiO_2-g-PEI MMMs were 104.11LMH and 99.00%. The SiO_2 wt % of 0.8447%, MBV concentration of 98.18 ppm, and pH of 4 were the optimal parameters for the SiO_2 MMMs, while the optimal parameters for SiO_2-g-PEI MMMs were SiO2-g-PEI wt. % of 0.93%, MBV concentration of 22.7 ppm, and pH of 4.79 for eliciting the optimum response.

* Corresponding author.
E-mail address: qusay.f.abdulhameed@uotechnology.edu.iq (Q.F. Alsalhy).

https://doi.org/10.1016/j.jmrt.2023.04.247

1. Introduction

Pollution levels in water have increased due to a shortage of freshwater supplies and the large streams of industrial effluent and sewage, and this dilemma has expanded into a major concern that threatens mankind and life on the planet. Population growth, particularly in emerging nations, industrial development, and economic growth necessitate the employment of safe and sustainable technology to solve this global problem. Industrial water treatment, which involves extracting pollutants and purifying water from them, is a required and difficult procedure in many sectors, including leather, tanning, dyes, petrochemical, and pharmaceuticals [1]. One of the fundamental concerns in these streams is the introduction of harmful pharmaceutical substances (PhCs) into the ecosystem, which eventually requires immediate response [2]. PhCs are commonly produced by a number of industries, including medicine, animal husbandry, aquaculture, and everyday life. PhCs have become a significant topic of worry in recent years due to a lack of regulatory limits for their discharge into surface water bodies. According to recent research, the manufacturing and administration of PhCs might vary between states and throughout time, from year to year. Furthermore, as the world's population ages and living standards improve, their use is projected to rise in the upcoming years [3]. According to various studies [4–7], PhCs were identified in surface water at quantities ranging from ng/L to μg/L, and in wastewater and groundwater at values ranging from ng/L to mg/L [8,9]. Because of their high chemical stability, bioaccumulation propensity, limited biodegradability, and mutagenesis effects, PhCs are harmful to the environment even at extremely low concentrations [10,11]. There are several reliable ways for industrial wastewater treatment. The most widely utilized treatment techniques for organic pollutant consist of membrane technique, adsorption, electrochemical, flocculation, chemical precipitation and ion exchange. Among these techniques, membrane separation based on pressure-driven is utilized in a variety of applications as a selective barrier between two parts. Membranes have been extensively investigated in recent studies for the efficient removal of pharmaceuticals. When compared to other conventional separation processes, they provide environmental safety, high separation efficiency, low energy consumption, easy maintenance, no need for chemicals, excellent permeate quality, and operating temperatures that are moderate making them an excellent option for wastewater treatment, either alone or as part of a hybrid process [12–18]. Despite the fact that membrane approaches play a significant role in wastewater treatment, fouling limits their usage in some applications. Fouling lowers water transport across the membrane and deteriorates other functional aspects of the membrane surfaces, increasing energy consumption and lowering life of membrane. Another difficulty is the tradeoff between permeability and selectivity. It is difficult to improve one without sacrificing the other for the currently used polymeric membranes [16,18]. It is therefore recommended to modify the surface of the membranes to provide the required specific characteristics [19]. An increasing amount of attention has been dedicated to surface modification because the skin layer controls interactions with hydrophobic foulants during membrane separation, which is a surface-dependent process. Membrane modification is the process of changing a membrane's surface properties using a particular chemical or physical method in order to increase the membrane's hydrophilicity and lessen its susceptibility to foul. For this purpose, dipping, coating, plasma, and blending have all been widely used [20,21]. The incorporation of nanoparticles in polymeric matrices, was found to improve membrane permeability and rejection capabilities, such as tungsten oxide ($WO_{2.89}$) [18], zinc oxide (ZnO) [22–24], Metal–Organic Frameworks (MOFs) [22], multi-walled carbon nanotube grafted graphene oxide (MWCNT-g-GO) [25], multi-walled carbon nanotube MWCNT and alumina [26], the mobile composition of matter (MCM-41) mesoporous [27,28], functionalized-MWCNTs and GO [29], titanium oxide (TiO_2) [22,30], titanium dioxide (TiO_2) functionalized with amino or vinyl silane [31], Ag–ZnO composite [32], Ag–SnO_2 [33,34], Boric Oxide-Reinforced Silver-Based [35], nanocrystalline $Cu_{25}Mo$ [36], antimony tin oxide (ATO) [22], silicon dioxide (SiO_2) functionalized with amino silane [37], SiO_2 or TiO_2 functionalized with amino silane [38], and GO [39,40]. Among these nanomaterials, silicon dioxide nanoparticles (SiO_2 NPs) are less harmful and ecologically inert than other nanoparticles. Because of desirable properties such as tiny particle size, narrow particle size distribution, a significant number of hydroxyl groups, and unsaturated residual bonds on its surface, SiO_2 NPs can have a positive impact on membrane performance. Meanwhile, the nanoparticles aggregation on the membrane surface is a problem inherent with zero-dimension nanomaterials. Agglomeration happens when NPs concentrations above a certain threshold, clogging membrane pores and altering membrane permeate flow [41–44]. Surface modification of nanoparticles *via* polymer chain grafting may be a useful way for dealing with the limitations of these weak interactions [45]. Polyethylenimine (PEI) has been shown to have distinct properties such as biocompatibility, hydrophilicity, and chemical activity, making it an appealing macro void formation agent [46–48]. Many efforts have been made to enhance the performance of MMMs in order to obtain greatest permeate flux, solute rejection, and processing lifespan, which necessitates determining the best operating conditions for this process. Many factors, such as pH, feed solute concentration, embedding material content, and so on, have been chosen as suitable operating conditions. Kadhim et al. [28] investigated the influence of the operating parameters, such as the feed pH values, MCM-41, and the feed dye concentration for each of the two studied dyes, acid black 210 (AB-210) and rose bengal (RB). An MCM-41 content of nearly 0.8 wt% in the casting solution, feed dye concentration of 10 ppm for the studied dyes, and feed pH of 3 for the RB dye was found to be the optimal parameters for eliciting the response. The pH had no significant influence on the response for the AB-210 dye, while the pH shows some minor effects on response with the RB dye. Response surface methodology (RSM) may be used to increase the performance of operations on the response since it includes numerous statistical operations required for the response [49]. When compared to traditional procedures that examine the effects of one parameter at a time in a series of experimental trials [50], this method analyzes the effect of

variables and their interactions in a more robust and complete manner [50–54].

The aim of this work was to investigate the optimization of ultrafiltration process operating parameters with SiO_2 and novel SiO_2-grafted-PEI (SiO_2-g-PEI) MMMs using response surface methodology (RSM) and analysis of variance (ANOVA). The current work studied the optimization of various operating parameters using MINITAB®18 software (i.e., SiO_2 and novel SiO_2-g-PEI NPs [0.7–1%], pH value [4–10], and Mebeverine HCl (MBV) feed concentration [10–100 ppm]) in relation to the membrane permeability and MBV rejection (%). Furthermore, the interaction effects of operational parameters to make the performance of PES-NPs membranes great as possible were investigated. Mebeverine HCl (MBV), "4-[ethyl (4-methoxy-α-methylphenethyl) amino] butylveratrate hydrochloride" (see Fig. S1), is a general antispasmodic that works directly on the smooth muscle of the gastrointestinal tract. MBV is a relaxant that is extensively used in the treatment of gastrointestinal spasmodic disorders such as irritable bowel syndrome, as well as a variety of other maladies involving the vascular system, gastrointestinal tract, and genitourinary tract. It has the chemical formula $C_{25}H_{35}NO_5 \cdot HCl$, and molecular weight of 466 Da [55]. MBV was selected based on the high-risk characterization ratio (RCR), yearly chemical consumption, and worldwide reports of incidence [15]. Risk characterization ratios (RCRs) were used to rank the PhCs, with the greatest RCRs indicating drugs with the highest priority. Based on all risk comparisons; MBV is one of three PhCs that have RCR >1 in three Iraqi cites Baghdad, Basrah, and Mosul as reported by Al-Khazrajy and Boxall [56]. To the best of the author's knowledge, no trial involving such optimization nanostructure for mixed matrix membranes has been documented in the literature for treatment of Mebeverine HCl (MBV) from pharmaceutical wastewater.

2. Experimental work

2.1. Materials

The main polymer was polyethersulfone (PES) (MW = 30000 g/mol) was obtained from Solvay Advanced Polymers (Belgium) for membrane preparation, polyvinylpyrrolidone (PVP, MW = 30000 g/mol) as a membrane pore-former, N, N dimethylformamide (DMF, greater than 99%), anhydrous toluene (99%), and isopropanol were purchased from (Thomas Baker). Mebeverine hydrochloride (MBV) with MW = 466 g/mol was given by Global Calcium Private Limited Company. Hyper branched polyethylenimine (PEI) (MW = 25000 g/mol) and 3-chloropropyle triethoxysilane (CPTES, 95%, $C_9H_{21}ClO_3Si$, MW = 240.8 g/mol) were acquired from Sigma Aldrich, Merck, USA (India). SiO_2 nanoparticles with typical particle sizes of 15–20 nm were obtained from US Research Nanomaterials Inc. (USA).

2.2. Modification of SiO_2 NPs process with polyethylenimine

Before grafting with PEI hydrophilic polymer, the SiO_2 NPs was functionalized with CPTES as described in our previous work [47]. In brief, to obtain (SiO_2-CPTES), the SiO_2 NPs' surface was firstly functionalized with CPTES. After that, the PEI grafting process was conducted *via* SiO_2-CPTES dispersion in the PEI polymer solution. PEI was grafted onto the surface of silica NPs by coupling mode, yielding SiO_2–g–PEI NPs as a new composite material.

2.3. Mixed matrix membranes (MMMs) flat sheet manufacture

Nine MMMs were fabricated *via* the classical non induced phase separation technique (NIPS). The total composition of the membranes is displayed in Table S1 [47]. Initially, the PES was dried in an oven at 60 °C for 3 h to eliminate the moisture content. Various amounts ratios (0.7–1 wt %) of SiO_2 and SiO_2-g-PEI were individually dispersed in DMF solvent and PVP and the mixture was sonicated for 1 h to achieve homogeneity. Following that, the PES was added to the mixture and mixed for 24 h to obtain complete polymer dissociation. Air bubbles were removed by leaving the casting solution quiescent at room temperature. The dope solutions were cast at a thickness of 200 μm using an automatic film applicator (AFA-IV, China). For deposition, the polymer films were immersed in a coagulation bath (distilled water) at 25 ± 1 °C. The membranes were rinsed thoroughly and immersed in distilled water for 48 h to ensure there is no residual solvent. Afterward, the membranes were transferred and submerged in a 25% glycerol solution for 48 h to prevent the membrane structure from collapsing.

The specification of all modified and unmodified membranes such as contact angle, thickness, porosity, and mean pore radius were presented in Table 1.

2.4. Mixed matrix membranes performance

The performance of the membrane (pristine and MMMs) was evaluated using a cross-flow membrane filtration lab-scale unit at room temperature (25 ± 1 °C), as shown in Fig. 1. Before measuring pure water flux, all membranes were pre-compacted at 4 bars for 1 h to achieve constant pure water flux (PWF). The pressure was then decreased to 2 bar, and the volume of permeate was measured. The permeation flux was computed using Eq. (1) below:

$$J = \frac{V}{A \times t} \quad (1)$$

Where: J, V, A, and t is the permeable water flux (L/m^2 hr) (LMH); the collected permeate volume (L); the membrane effective area (m^2), and the collected time (h) respectively.

The mebeverine hydrochloride (MBV) solution rejection test was carried out at various concentrations (10, 30, 50, 70, and 100 ppm). The influence of the MBV-simulated wastewater solution pH on the performance of the MMMs was also studied in this work. The quantities of (MBV) in the feed and permeate fluxes were measured using high-performance liquid chromatography (HPLC) (SYKAM-Germany). The rejection % of (MBV) was computed using Eq. (2) [25,57]:

$$R\% = \left(1 - \frac{C_p}{C_f}\right) \times 100 \quad (2)$$

Table 1 – Effect of SiO_2 and SiO_2-g- PEI wt % on contact angle, thickness, porosity, and mean pore radius of MMMs.

Membrane Code	Thickness[a] ± STDV (μm)	Porosity ± STDV (%)	Contact angle ± STDV (°)	mean pore radius (nm) ± STDV
SiO_2				
D0	102.70 ± 1.00	62.82 ± 0.61	65.60 ± 1.52	8.10 ± 0.21
D0.7	105.80 ± 1.65	69.32 ± 1.08	61.99 ± 2.50	9.20 ± 0.20
D0.8	95.66 ± 1.00	72.77 ± 0.76	62.00 ± 2.50	10.74 ± 0.15
D0.9	92.70 ± 3.20	77.86 ± 2.69	58.92 ± 1.83	13.30 ± 0.66
D1	84.26 ± 1.00	68.20 ± 0.81	63.56 ± 2.46	7.60 ± 0.12
SiO_2-g-PEI				
D0	102.70 ± 1.00	62.82 ± 0.61	65.60 ± 1.52	8.10 ± 0.21
DS0.7	94.80 ± 0.76	82.75 ± 0.66	55.56 ± 2.45	12.22 ± 0.14
DS0.8	92.29 ± 0.88	84.92 ± 0.81	53.84 ± 2.78	12.25 ± 0.18
DS0.9	81.20 ± 1.54	89.96 ± 1.71	49.04 ± 1.84	13.55 ± 0.41
DS1	79.70 ± 1.00	84.86 ± 1.06	54.04 ± 3.05	10.50 ± 0.21

[a] The thickness of the membranes was measured by using an FESEM device.

Where: R, C_p, and C_f is the rejection of MBV; the MBV concentration in the permeate solution (ppm); and the MBV concentration in the feed solution (ppm) respectively.

3. Results and discussion

3.1. MMMs filtration cross-flow evaluation

Compared to the pristine membrane, each MMM displayed a greater pure water flux (PWF). The permeability characteristics were significantly affected by the incorporation of nanoparticles, even at low loading levels. The results revealed that the water flux increased from 20 ± 0.148 LMH for the original membrane (D0) to 30 ± 0.12 LMH by adding 0.7% SiO_2 NPs. After the addition of SiO_2 NPs, PWF continued to show a significant increase, reaching its greatest value for D0.9 with an 88 ± 0.66 LMH. Accordingly, as previously demonstrated in this work, the increasing trend of PWF was consistent with hydrophilicity measures, MMMs pore size, and porosity. The PWF has decreased to roughly 25 ± 0.14 LMH with the addition of 1% SiO_2 NPs. Due to the large concentration of SiO_2 NPs, the pore has become blocked, which is the cause of the PWF reduction [58]. The water flux rose to 82 ± 1.63 LMH after 0.7 wt % SiO_2-g- PEI NPs were added, compared to 20 ± 0.148 LMH for a virgin membrane. After the embedding of NPs, PWF showed a significant rise that peaked at a value that was more than seven times higher (140 ± 1.28 LMH) for the DS0.9 membrane than for the D0 membrane. However, adding a larger concentration of 1% of modified SiO_2 NPs to MMMs led to a decrease in the PWF to roughly 82.1 ± 0.66 LMH, see Table 2.

3.2. Process modeling and optimization

Response surface methodology (RSM) is a combination of mathematical and statistical approaches that can be used to model and analyze problems in which a response of interest is affected by multiple parameters and the goal is to optimize this response. Response surface methodology (RSM) can be used to increase the performance of operations on the

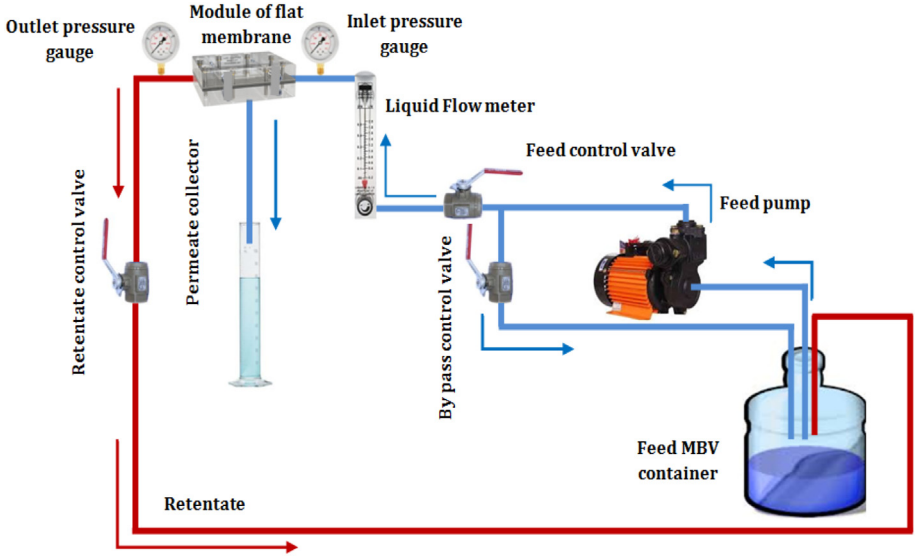

Fig. 1 – Cross-flow filtration system schematic diagram.

Table 2 – Mixed matrix membrane pure water permeate flux (25 ± 1 °C, 2 bars and pH = 6).

Membrane Code	PWF ± STDV LMH	Membrane Code	PWF ± STDV LMH
D0	20.08 ± 0.15	D0	20.08 ± 0.15
D0.7	30.07 ± 0.12	DS0.7	82.00 ± 1.63
D0.8	49.07 ± 0.69	DS0.8	89.03 ± 1.40
D0.9	88.08 ± 0.65	DS0.9	140.05 ± 1.28
D1	25.07 ± 0.14	DS1	82.15 ± 0.67

response since it incorporates several statistical operations required for the response [49]. When compared to traditional procedures that examine the effects of one parameter at a time in a series of experimental trials [45], this method analyzes the effect of variables and their interactions in a more robust and complete manner [50–54].

MINITAB®18 software was used to conduct the analyses. The current work studied the optimization of various operating parameters (e.g., pH value [4–10], SiO_2 and SiO_2-g-PEI NPs [0.7–1%], and MBV feed concentration [10–100 ppm]) in relation to the membranes' permeability and rejection %. Furthermore, the interaction effects of operational factors were investigated. Analysis of variance ANOVA is a statistical model that is used to examine the variations between various parameters in a regression study; particularly, this method is used to explain the influence of independent variables on dependent variables. ANOVA can be used to more precisely choose the best set of operational parameters by examining the relative significance of the variables [1]. Table 3 displays the experimental values and parameter symbols.

A set of tests were performed using the UF membrane technique, each altering one factor to determine the necessary set of operational parameters while holding the other factors constant. The goal of the optimization method central composite design (RSM) is to determine the effect of independent (predictor) factors on the permeate flux and rejection % (response) mechanism.

3.3. *Statistical modeling analysis by ANOVA*

MINITAB®18 was utilized to conduct ANOVA analyses, with a 5% relevance threshold necessary to investigate a variable crucial to the execution process. The ANOVA results for permeate flux and rejection % as a function of SiO_2 or SiO_2-g-PEI wt. %, MBV concentrations, and pH values is shown in Tables (S2, and S3), where each one of the predictor variables in the layout of design has a p-value in the ANOVA table. The differences are statistically significant when the p-value is less than 5% [1]. The analysis of the results was utilized to predict a mathematical expression. The regression model equation for permeate flux and rejection% are expressed as Eqs (3)–(6) for SiO_2 and SiO_2-g-PEI MMMs in terms of actual factors, respectively.

$$PF_1 = -633.8 + 1691\,N - 0.137\,C - 7.05\,pH - 1018.5\,(N)^2 - 0.001008\,(C)^2 + 0.123\,(pH)^2 + 0.049\,N\,x\,C + 3.22\,NxpH + 0.01209\,C\,x\,pH \quad (3)$$

$$Rej_1\% = 42.4 + 44.8\,N + 0.2378\,C + 0.378\,pH - 17.2\,(N)^2 - 0.000085\,(C)^2 - 0.0191(pH)^2 - 0.1335\,N\,x\,C + 0.464\,N\,x\,pH - 0.00247\,C\,x\,pH \quad (4)$$

$$PF_2 = -788.2 + 2343\,N - 0.541\,C - 24.38\,pH - 1406\,(N)^2 + 0.00042\,(C)^2 + 0.889\,(pH)^2 + 0.231\,Nx\,C + 7.53\,NxpH + 0.00458\,C\,x\,pH \quad (5)$$

$$Rej_2\% = -150.9 + 505.9\,N + 0.2423\,C + 2.25\,pH - 264.4\,(N)^2 - 0.00042\,(C)^2 - 0.0999\,(pH)^2 - 0.1759\,Nx\,C - 0.422\,NxpH - 0.00102\,C\,x\,pH \quad (6)$$

Where: PF_1 and PF_2 are permeate flux (LMH) of SiO_2 MMMs and SiO_2-g-PEI MMMs respectively; Rej_1% and Rej_2% are rejection % of SiO_2 MMMs and SiO_2-g-PEI MMMs respectively; N, C, and pH are SiO_2 or SiO_2-g-PEI NPs wt. %, MBV concentration (ppm), pH of MBV solution, respectively.

The correlation coefficient R^2 for the permeate flux and rejection% model were found equal to 97.64% and 98.33% for SiO_2 MMMs respectively, and R^2 for the permeate flux and rejection% model were 96.38% and 99.39% for SiO_2-g-PEI MMMs respectively. Moreover, the R^2-adjusted values are 95.52% and 96.83% for SiO_2 MMMs respectively, 93.13% and 98.84% for SiO_2-g-PEI MMMs respectively which are sufficiently high and in good agreement with the R^2 values. As a consequence, the findings show that the permeate flux and

Table 3 – Values and codes of the experimental variables at various levels of SiO_2 and SiO_2-g-PEI MMMs.

Parameters	Code	Unit	Low level	High level
SiO_2				
SiO_2 NPs	N	wt. %	0.7	1
MBV concentration	C	ppm	10	100
pH of solution	pH	Unit less	4	10
Permeate flux	PF_1	LMH	Target	
Rejection %	Rej_1%	%	Target	
SiO_2-g-PEI				
SiO_2-g-PEI NPs	N	wt. %	0.7	
MBV concentration	C	ppm	10	
pH of solution	pH	Unit less	4	
Permeate flux	PF_2	LMH	Target	
Rejection %	Rej_2%	%	Target	

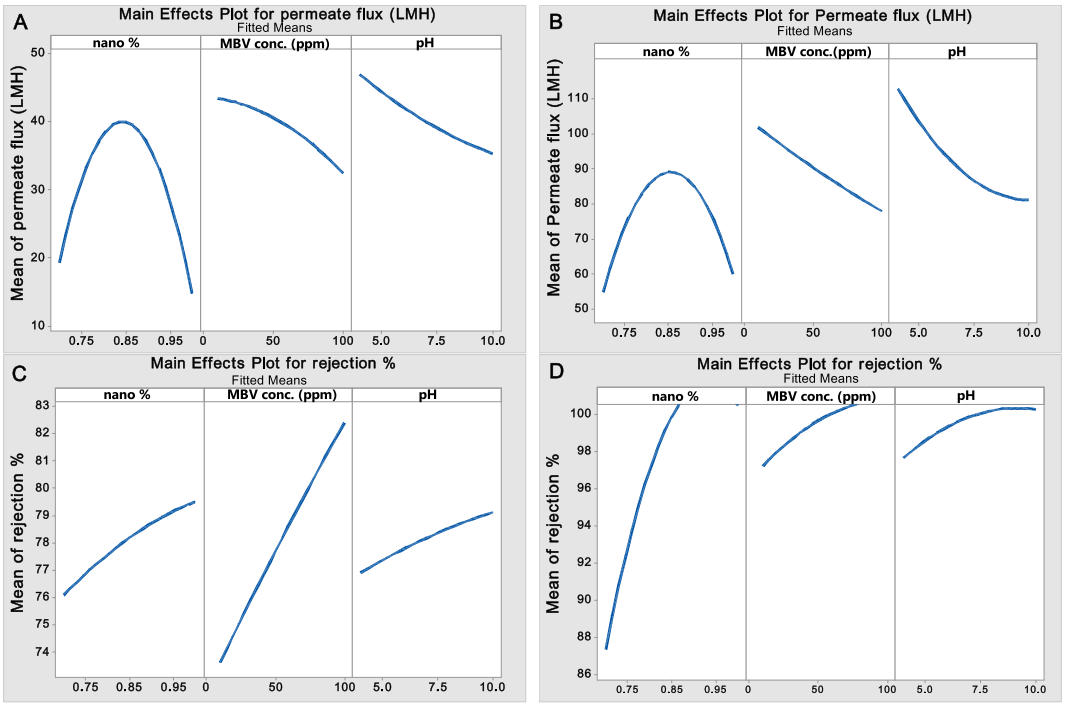

Fig. 2 – Plot of main effect of the MBV concentration, pH, and nano wt% on the permeate flux using (A) SiO_2 MMMs (B) SiO_2-g-PEI MMMs and rejection % of MBV using (C) SiO_2 MMMs (D) SiO_2-g-PEI MMMs.

rejection% model is statistically valid and can be used to forecast the performance of UF MMMs with high accuracy. The regression result of the permeate flux and rejection% models indicates that the model can fitted the data represented well and with reasonable accuracy [54].

3.4. *Effect of pareto chart*

Fig. S2 shows a Pareto chart of the standardized effects for MBV permeate flux and rejection % of SiO_2 MMMs and SiO_2-g-PEI MMMs. The figure shows the effect of different variables on MBV permeate flux and rejection%, such as nano % (factor A), MBV concentration, ppm (factor B), MBV solution pH (factor C), and many interaction factors. As a result, for every coefficient's regular impact value to be consistently relevant at the 5% level, it must be bigger than the critical value of 2.23. As shown in Fig. S2(A), the term (AA), which reflects the quadratic impact, demonstrates the significance of the SiO_2 wt % content, and the lower significant influence of the terms (C, B, and A) on permeate flux, also the terms (AA) which show almost the significant of SiO_2-g-PEI wt % and the lower significant influence of the terms (C, B, and CC) on permeate flux as shown in Fig. S2(B). Fig. S2(C) shows that the term (B) demonstrates the significance of the MBV concentrations, and the lower significant influence of the terms (A, C, and AB) on rejection% of SiO_2 MMMs, while the terms (A) which show the significant of SiO_2-g-PEI wt %, and the lower significant influence of the terms (AA, B, C, and AB) on rejection % of SiO_2-g-PEI MMMs as shown in Fig. S2(D). All results confirm the ANOVA results analysis in term of P-value where all factors with significant influence have value less than 0.05.

3.5. *Main effects plot*

Fig. 2 illustrates the main effects plot for the MBV permeate flux and rejection%. The main effects plot as shown in Fig. 2(A) indicates that the SiO_2 wt% content was the most essential element on permeate flux, followed by the pH and MBV concentration, and SiO_2-g-PEI wt% content and pH was the most influential factors on permeate flux, followed by the MBV concentration as shown in Fig. 2(B).

The main effects plot as shown in Fig. 2(C) indicates that the MBV concentration was the most influential factor on rejection%, followed by SiO_2 wt% content and pH, and SiO_2-g-PEI wt% content was the most influential factors on rejection %, followed by the MBV concentration and pH as shown in Fig. 2(D).

3.6. *Variables interaction plot*

The graphs of interaction for all process variables and their effect on the permeate flux and rejection % is illustrated in Fig. 3. The interaction plot between the SiO_2/or SiO_2-g-PEI wt % and MBV concentration show that, the maximum permeate flux was observed for SiO_2/or SiO_2-g-PEI wt% of approximately 0.85 wt% in the dope casting solution at 10 ppm, and the minimum permeate flux was showed for a 0.7 wt% at a dye concentration of 100 ppm, but the SiO_2-g-PEI MMMs have larger permeate flux. The plot of interaction between the MBV concentration and SiO_2/or SiO_2-g-PEI wt% showed that as the concentration increased, the permeate flux decreased for all SiO_2/or SiO_2-g-PEI wt% as shown in Fig. 3(A and B).

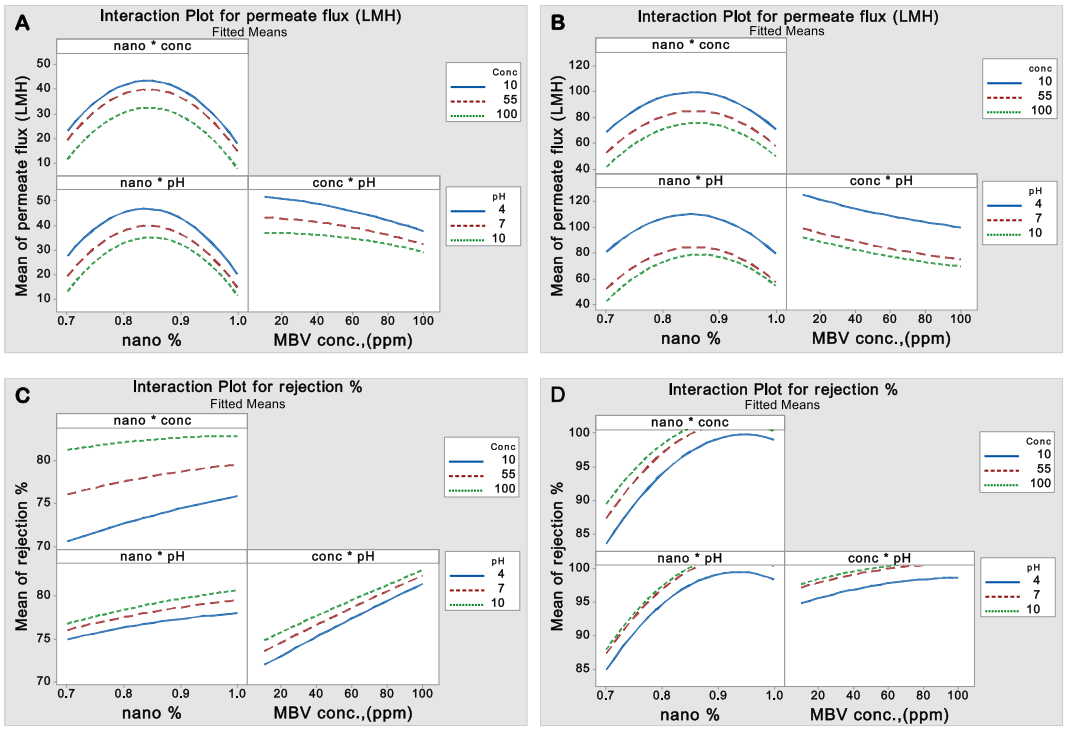

Fig. 3 – Interaction plots of the effect of MBV concentration, pH, and nano wt% effect on the permeate flux using (A) SiO_2 MMMs (B) SiO_2-g-PEI MMMs and rejection % of MBV using (C) SiO_2 MMMs (D) SiO_2-g-PEI MMMs.

However, the interaction plot between MBV feed concentration and pH revealed that the permeate flux of all pH of solutions decreased importantly as feed concentration increased. At an MBV dosage of 10 ppm, maximum permeates flux was found for all feed pH levels. The graph clearly shows that the interactions for SiO_2-g-PEI MMMs have higher permeate flux than SiO_2 MMMs.

The interaction plot between the SiO_2/or SiO_2-g-PEI wt% and MBV concentration shows that the maximum rejection% was observed for SiO_2/or SiO_2-g-PEI wt% of about 1 wt% in the casting solution at 100 ppm, and the lowest rejection% was observed for a 0.7 wt% at a dye concentration of 10 ppm, but the SiO_2-g-PEI MMMs have approximately complete rejection %. The plot of interaction between the MBV concentration and SiO_2/or SiO_2-g-PEI wt% showed that as the concentration increased, the rejection% increased for all SiO_2/or SiO_2-g-PEI wt% as shown in Fig. 3(C and D).

However, the interaction plot between MBV feed concentration and pH revealed that the rejection% of all pH solutions increased significantly as feed concentration increased with minimum influence for SiO_2-g-PEI MMMs. At an MBV dosage of 100 ppm, maximum rejection% was found for all feed pH levels. The graph clearly shows that the interactions for SiO_2-g-PEI MMMs have complete rejection% compared with SiO_2 MMMs.

3.7. *Response surface analysis*

The permeate flux and rejection % of MBV response can be characterized as a solid in three-dimensional space, as shown in Fig. 4, where the permeate flux and rejection % are plotted against the two variables. The response surface graph's main objective is to identify the optimal operation variables, which are represented by the MBV concentration, pH value, and nano wt % (either SiO_2 or SiO_2-g-PEI) which results in the highest permeate flux and rejection % of MBV solution. The MBV permeate flux response showed that decreasing pH and decreasing feed concentration resulted in increased permeate flux at a constant 0.85 wt % nano (either SiO_2 or SiO_2-g-PEI), as shown in Fig. 4 (A and B). The maximum permeate flux record more than 40 LMH with 0.85 wt% of SiO_2 NPs addition compared with more than 90 LMH with 0.85 wt% of SiO_2-g-PEI NPs addition when kept the pH at 7. For SiO_2-g-PEI NPs MMMs, the increased of pH and MBV concentration led to a decreased permeate flux but with lower significant.

The MBV rejection % response showed that decreasing pH and decreasing feed concentration resulted in decreased rejection % at a constant 0.85 wt % nano (either SiO_2 or SiO_2-g-PEI), as shown in Fig. 4(C and D). The maximum rejection % record about 80% with 1 wt % of SiO_2 NPs addition compared with more 99.99% with 1 wt% of SiO_2-g-PEI NPs addition when kept the pH at 7. The increase of pH and MBV concentration have a more significant effect on the rejection % for the SiO_2 MMMs compared with a no effect on the rejection % for SiO_2-g-PEI MMMs.

3.8. *Predicted fitted line plot*

A Minitab prediction of permeate flux and rejection % was created by a linear regression function (MINITAB®18). The predicted and experimental values of permeate flux and MBV rejection % are shown in Fig. 5.

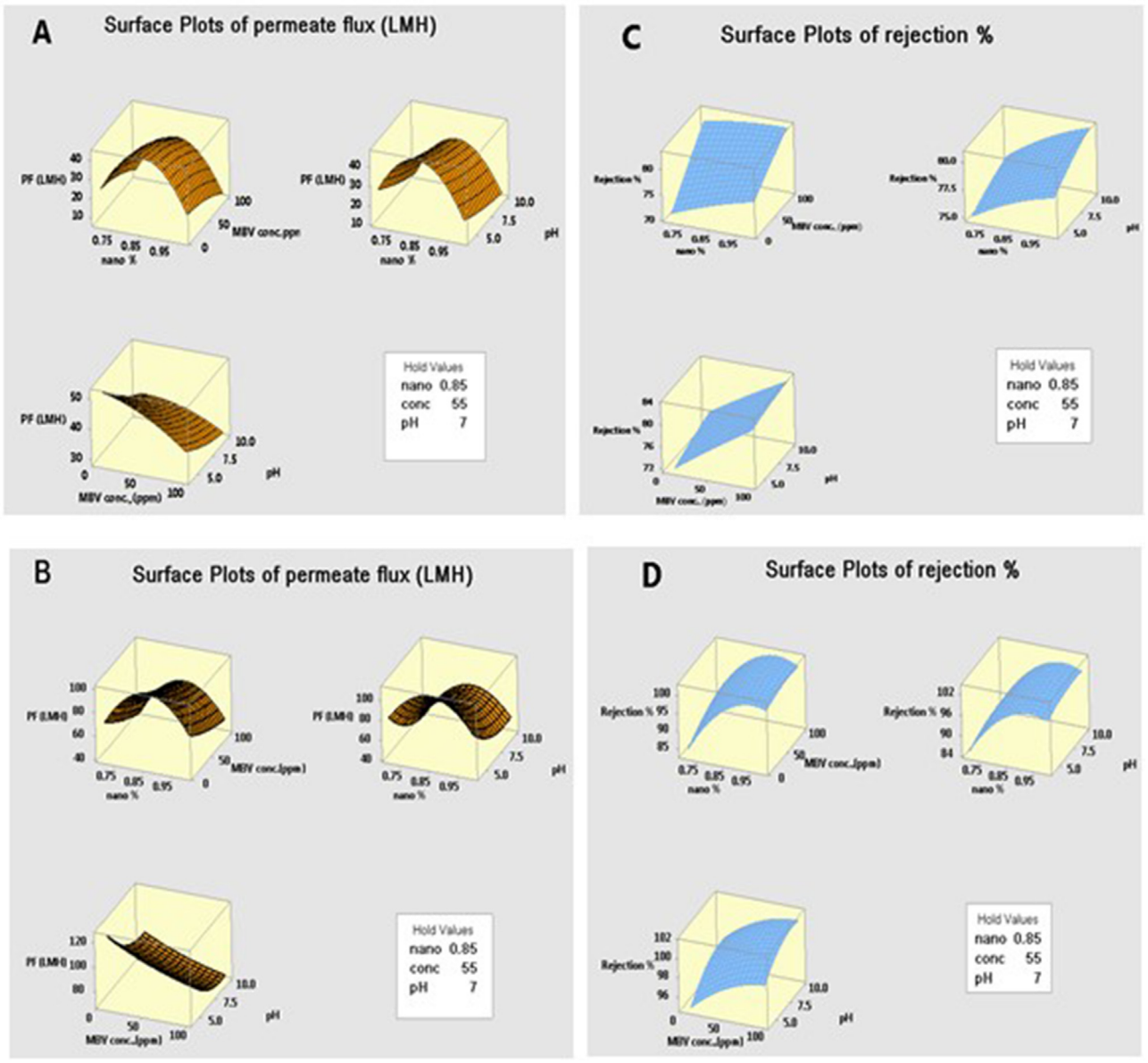

Fig. 4 – 3D response surface plots of the effect of MBV concentration, pH, and nano wt% on the permeate flux using (A) SiO_2 MMMs (B) SiO_2-g-PEI MMMs and rejection % of MBV using (C) SiO_2 MMMs (D) SiO_2-g-PEI MMMs.

In order to evaluate the validation of the model, the predicted and experimental values were compared as shown in Tables S4 and S5. As can be seen, the experimental and predicted values of permeate flux and rejection % of SiO_2 MMMs and SiO_2-g-PEI MMMs are mathematically in good agreement. These results and the high R-square (i.e., 97.6% and 98.3% for permeate flux and rejection %) of SiO_2 MMMs and (i.e., 96.4% and 99.4% for permeate flux and rejection %) of SiO_2-g-PEI MMMs demonstrate the model's significant potential for permeate flux and rejection % prediction and optimization [59].

3.9. *Optimization of the MMMs permeate flux and rejection %*

The desire function approach is one of the most often employed techniques in the vast field of applied science and engineering for the optimization of multiple response processes. With this approach, the individual desirability of several responses is combined into a single number with a range from 0 to 1.0. Since a value of 1 represents the optimum situation, values that are closer to 1 are preferred when defining the ideal operating circumstances [59]. By using a response optimizer design with various three variables, as observed in Table 4, if concurrently acceptable permeate flux and rejection % values are taken into account, the permeate flux and rejection % of SiO_2 MMMs is 38.27 LMH and 81.26% which achieved at SiO_2 wt % of 0.8447%, MBV concentration of 98.18 ppm, and pH of 4, while the permeate flux and rejection % of SiO_2-g-PEI MMMs is 104.11 LMH and 99.00% which achieved at SiO_2-g-PEI wt % of 0.93%, MBV concentration of 22.7 ppm, and pH of 4.79.

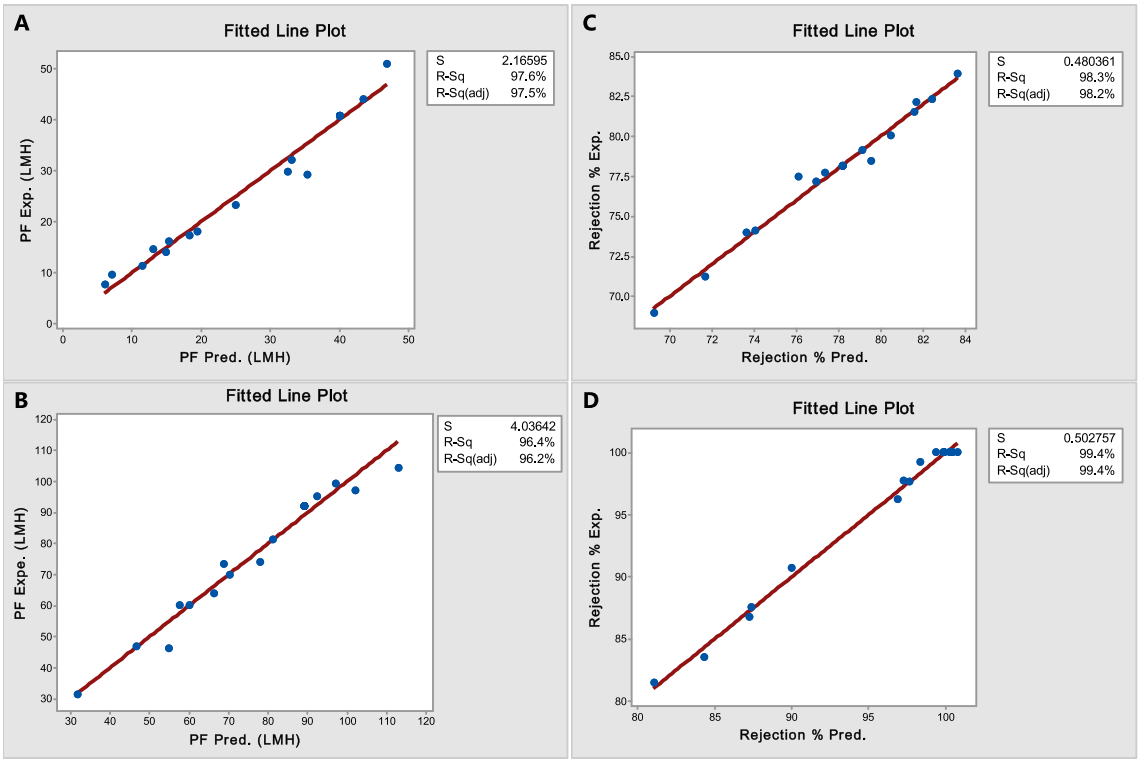

Fig. 5 – Predicted versus experimental values of the permeate flux using (A) SiO_2 MMMs (B) SiO_2-g-PEI MMMs and rejection % of MBV using (C) SiO_2 MMMs (D) SiO_2-g-PEI MMMs.

Table 4 – Predicted and experimental values of the MMS: permeate flux and rejection % at optimized conditions.

MMMs	Nano (%)	MBV conc. (ppm)	pH	PF (LMH) Pred.	PF (LMH) Exp.	Error (%)	Rej. (%) Pred.	Rej. (%) Exp.	Error (%)	Composite desirability
SiO_2 MMMs	0.8447	98.18	4	38.27	40.10	4.56	81.26	84.70	4.06	0.800
SiO_2-g-PEI MMMs	0.93	22.7	4.79	104.11	101.64	2.43	99.00	99.99	0.99	0.972

When using fabricated MMMs with varied modified SiO_2 NPs concentrations at different MBV solution concentrations, the permeate flux and rejection % increases. This increase can be attributed to the hydrophilicity and morphological characteristics of the MMMs.

3.10. *Validation of the optimum conditions*

The permeate flux and rejection % experiments were carried out at the optimum operating conditions suggested by the model to validate it. It should be noted from Table 4, that only 4.56% and 2.43% error % was found between the predicated permeate flux (38.27 LMH), (104.11 LMH) and experimental value (40.10 LMH), (101.64 LMH) for SiO_2 MMMs and SiO_2-g-PEI MMMs, respectively, while the error % was 4.06% and 0.99% between the predicted rejection % (81.26), (99) and experimental value (84.70), (99.99) for SiO_2 MMMs and SiO_2-g-PEI MMMs, respectively. The low percentage error confirms that the developed RSM model is significant and applicable [60].

4. Conclusions

This study compared the effects of embedded of SiO_2 and SiO_2-g-PEI nanoparticles on a flat sheet PES mixed matrix membranes for the removal of mebeverine hydrochloride from simulated pharmaceutical wastewater. Using mebeverine hydrochloride, all pristine and mixed matrix membranes were thoroughly described in terms of permeate flux and separation factor. To enhance the process' effectiveness on a bigger scale, response surface methodology (RSM) and analysis of variance (ANOVA) were utilized as mathematical and statistical approaches. The effect of operating parameters on the permeate flux and MBV rejection % of PES/SiO_2 and PES/SiO_2-g-PEI NPs flat sheet mixed matrix membranes in the ultrafiltration process were optimized. The three parameters identified as having the most influence on the permeate flux and MBV rejection were the SiO_2 or SiO_2-g-PEI NPs wt %, MBV concentration, and solution pH values. The experimental design allowed for studying the effect of three levels for MBV.

These experiments found that the SiO_2 or SiO_2-g-PEI NPs wt % content and pH were the most significant parameters to influence the permeate flux. In contrast, the SiO_2-g-PEI NPs wt % was the most significant parameters to influence the MBV rejection % for SiO_2-g-PEI MMMs, while the MBV concentration was the most significant parameters to influence the MBV rejection % for SiO_2 MMMs. The permeate flux and rejection % were studied using Minitab 18. A mathematical model to calculate the permeate flux and rejection % was established. The results show a combined effect of variables on permeate flux and rejection %. The optimized variables show that the permeate flux and rejection % of SiO_2 MMMs is 38.27 LMH and 81.26% which achieved at SiO_2 wt % of 0.8447%, MBV concentration of 98.18 ppm, and pH of 4, while the permeate flux and rejection % of SiO_2-g-PEI MMMs is 104.11 LMH and 99.00% which achieved at SiO_2 wt % of 0.93%, MBV concentration of 22.7 ppm, and pH of 4.79.

Related list of nomenclature

List of abbreviations; List of Greek symbols can be found among **Supplementary Information**.

Funding

The authors are thankful for the financial support from NRDIO Hungary (SNN 143949). Z. Németh would like to thank the Hungarian Academy of Sciences Bolyai János Research Scholarship Program.

Data availability statement

Not applicable.

Declaration of competing interest

The authors declare that they have no known competing financial interests or personal relationships that could have appeared to influence the work reported in this paper.

Appendix A. Supplementary data

Supplementary data to this article can be found online at https://doi.org/10.1016/j.jmrt.2023.04.247.

REFERENCES

[1] Al-Sultan AA, Khadim RJ, Al-Emami OH, Alsalhy QF, Majdi HS. Optimization of graphene oxide mixed matrix membrane for AB-210 dye removal. J. Ecological Eng 2022;23(9):115–27.

[2] Samer K, Al-Rimawi F, Mustafa K, Shlomo N, Bufo SA, Laura S, Gennaro M, Rafik K. Efficiency of membrane technology, activated charcoal, and a micelle-clay complex for removal of the acidic pharmaceutical mefenamic acid. J Environ Sci Health, Part A 2013;48:1655–62.

[3] Verlicchi P, Al Aukidy M, Zambello E. Occurrence of pharmaceutical compounds in urban wastewater: removal, mass load and environmental risk after a secondary treatment—a review. Sci Total Environ 2012;429:123–55.

[4] Kasprzyk-Hordern B, Dinsdale RM, Guwy AJ. The occurrence of pharmaceuticals, personal care products, endocrine disruptors and illicit drugs in surface water in South Wales, UK. Water Res 2008;42:3498–518. https://doi.org/10.1016/j.watres.2008.04.026.

[5] Huerta-Fontela M, Galceran MT, Ventura F. Occurrence and removal of pharmaceuticals and hormones through drinking water treatment. Water Res 2011;45:1432–42.

[6] Wu M, Xiang J, Que C, Chen F, Xu G. Occurrence and fate of psychiatric pharmaceuticals in the urban water system of Shanghai, China. Chemosphere 2015;138:486–93.

[7] Roberts J, Kumar A, Du J, Hepplewhite C, Ellis DJ, Christy AG, Beavis SG. Pharmaceuticals and personal care products (PPCPs) in Australia's largest inland sewage treatment plant, and its contribution to a major Australian river during high and low flow. Science of the Total Environment; 2015. p. 1–13. https://doi.org/10.1016/j.scitotenv.2015.03.145.

[8] Cabeza Y, Candela L, Ronen D, Teijon G. Monitoring the occurrence of emerging contaminants in treated wastewater and groundwater between 2008 and 2010. The Baix Llobregat (Barcelona, Spain). J Hazard Mater 2012;239– 240:32–9.

[9] Vázquez-Suñé E, Jurado A, López-Serna R, Carrera J, Petrovi M, Barceló D. Occurrence of 95 pharmaceuticals and transformation products in urban groundwaters underlying the metropolis of Barcelona, Spain. Environ Pollut 2013;174:305–15.

[10] Manu B, Mahamood S, Vittal H, Shrihari S. A novel catalytic route to degrade paracetamol by Fenton process. J. Res. Chem. Environ 2011;1:157–64.

[11] Bui TX, Choi H. Adsorptive removal of selected pharmaceuticals by mesoporous silica SBA-15. J Hazard Mater 2009;168:602–8.

[12] Puerari RC, Goncalves RA, Justino NM, Vicentini DS, Matias WG. The influence of amine-functionalized SiO_2 nanostructures upon nanofiltration membranes. Environ Nanotechnol, Monit Mang 2020;13:100287.

[13] Yoon Y, Westerhoff P, Snyder SA, Wert EC, Yoon J. Removal of endocrine disrupting compounds and pharmaceuticals by nanofiltration and ultrafiltration membranes. Desalination 2007;202:16–23.

[14] Verliefde ARD, Cornelissen ER, Heijman SGJ, Petrinic I, Luxbacher T, Amy GL, Bruggen BVD, Dijk JCV. Influence of membrane fouling by (pretreated) surface water on rejection of pharmaceutically active compounds (PhACs) by nanofiltration membranes. J Membr Sci 2009;330:90–103.

[15] Zhou JL, Zhang ZL, Banks E, Grover D, Jiang JQ. Pharmaceutical residues in wastewater treatment works effluents and their impact on receiving river water. J Hazard Mater 2009;166:655–61.

[16] Bellona C, Drewes JE, Xu P, Amy G. Factors affecting the rejection of organic solutes during NF/RO treatment—a literature review. Water Res 2004;38:2795–809.

[17] Kaykioglu MGG, Belgiorno V, Lofrano G. Removal of emerging contaminants from water and wastewater by adsorption process. 2012. https://doi.org/10.1007/978-94-007-3916-1_2. chap. 2.

[18] Abdullah RR, Shabeeb KM, Alzubaydi AB, Figoli A, Criscuoli A, Drioli E, Alsalhy QF. Characterization of the efficiency of photo-catalytic ultrafiltation PES membrane modified with tungsten oxide in the removal of tinzaparin sodium. Eng Technol J 2022;40(12).

[19] Al Aani S, Wright CJ, Atieh MA, Hilal N. Engineering nanocomposite membranes: addressing current challenges and future opportunities. Desalination 2017;401:1–15.
[20] Razmjou A, Mansouri J, Chen V, Lim M, Amal R. Titania nanocomposite polyethersulfone ultrafiltration membranes fabricated using a low temperature hydrothermal coating process. J Membr Sci 2011;380:98–113.
[21] Tran TD, Mori S, Suzuki M. Plasma modification of polyacrylonitrile ultrafiltration membrane. Thin Solid Films 2007;515:4148–52.
[22] Al-Maliki RM, Alsalhy QF, Al-Jubouri S, Salih IK, AbdulRazak AA, Shehab MA, Németh Z, Hernadi K. Classification of nanomaterials and the effect of graphene oxide (GO) and recently developed nanoparticles on the ultrafiltration membrane and their applications: a review. Membranes 2022;12:1043.
[23] Alsalhy QF, Ali JM, Abbas AA, Rashed A, der Bruggen BV, Balta S. Enhancement of poly(phenyl sulfone) membranes with ZnO nanoparticles. Desalination Water Treat 2013:1–13.
[24] Alsalhy QF, Al-Ani FH, Al-Najar AE, Jabuk SI. A study of the effect of embedding ZnO-NPs on PVC membrane performance use in actual hospital wastewater treatment by membrane bioreactor. Chem. Eng. Process.-Process. Intensificat. 2018;130:262–74.
[25] Sadiq AJ, Shabeeb KM, Khalil BI, Alsalhy QF. Effect of embedding MWCNT-g-GO with PVC on the performance of PVC membranes for oily wastewater treatment. Chem Eng Commun 2020;207:733–50.
[26] Jamed MJ, l Alanezi AA, Alsalhy QF. Effects of embedding functionalized multiwalled carbon nanotubes and alumina on the direct contact poly(vinylidene fluoride-cohexafluoropropylene) membrane distillation performance. Chem Eng Commun 2018;206(8):1035–57.
[27] Kadhim RJ, Al-Ani FH, Alsalhy QF. MCM-41 mesoporous modified polyethersulfone nanofiltration membranes and their prospects for dyes removal. Int J Environ Anal Chem 2021:1–22.
[28] Kadhim RJ, Al-Ani FH, Alsalhy QF, Figoli A. Optimization of MCM-41 mesoporous material mixed matrix polyethersulfone membrane for dye removal. Membranes 2021;11 414:1–20.
[29] Sadiq AJ, Awad ES, Shabeeb KM, Khalil BI, Al-Jubouri SM, Sabirova TM, Tretyakova NA, Majdi HS, Alsalhy QF, Braihi AJ. Comparative study of embedded functionalized MWCNTs and GO in Ultrafiltration (UF) PVC membrane: interaction mechanisms and performance. Int J Environ Anal Chem 2020:1–23.
[30] Al-Ani Faris H, Alsalhy QF, Raheem RS, Rashid KT, Alberto Figoli. Experimental investigation of the effect of implanting TiO2-NPs on PVC for long-term UF membrane performance to treat refinery wastewater. Membranes 2020;77:1–22.
[31] Abdel-Gawad NMK, El Dein AZ, Mansour DA, Ahmed HM, Darwish MMF, Lehtonen M. PVC nanocomposites for cable insulation with enhanced dielectric properties, partial discharge resistance and mechanical performance. High Volt 2020;5(4):463–71.
[32] Biyik S. Influence of type of process control agent on the synthesis of Ag-ZnO composite powder. Acta Phys Pol, A 2019;135(4):778–81. https://doi.org/10.12693/APhysPolA.135.778 (SCI).
[33] Biyik S. Effect of cubic and hexagonal boron nitride additions on the synthesis of Ag-SnO2 electrical contact material. J Nanoelectron Optoelectron 2019;14(7):1010–5. https://doi.org/10.1166/jno.2019.2592 (SCI-Exp).
[34] Biyik S, Aydin M. Fabrication and arc-erosion behavior of Ag-SnO2 electrical contact materials under inductive loads. Acta Phys Pol, A 2017;131(3):339–42. https://doi.org/10.12693/APhysPolA.131.339 (SCI).
[35] Biyik S, Arslan F, Aydin M. Arc-erosion behavior of boric oxide-reinforced silver-based electrical contact materials produced by mechanical alloying. J Electron Mater 2015;44(1):457–66. https://doi.org/10.1007/s11664-014-3399-4 (SCI).
[36] Biyik S. Characterization of nanocrystalline Cu25Mo electrical contact material synthesized via ball milling. Acta Phys Pol, A 2017;132(3):886–8. https://doi.org/10.12693/APhysPolA.132.886 (SCI).
[37] Abdel-Gawad NMK, Mansour DA, Darwish MMF, El Dein AZ, Ahmed HM, Lehtonen M. Impact of nanoparticles functionalization on partial discharge activity within PVC/SiO2 nanocomposites. IEEE 2nd International Conference on Dielectrics (ICD); 2018.
[38] Abdel-Gawad NMK, El Dein AZ, Mansour DA, Ahmed HM, Darwish MMF, Lehtonen M. Development of industrial scale PVC nanocomposites with comprehensive enhancement in dielectric properties. IET Sci Meas Technol 2019;13(1):90–6.
[39] Kadhim RJ, Al-Ani FH, Al-Shaeli M, Alsalhy QF, Figoli A. Removal of dyes using graphene oxide (GO) mixed matrix membranes. Membranes 2020;10:366.
[40] Al-Araji DD, Al-Ani FH, Alsalhy QF. The permeation and separation characteristics of polymeric membranes incorporated with nanoparticles for dye removal and interaction mechanisms between polymer and nanoparticles: a mini review. Eng Technol J 2022;40(11).
[41] Muhamad MS, Salim MR, Lau W. Preparation and characterization of PES/SiO2 composite ultrafiltration membrane for advanced water treatment. Kor J Chem Eng 2015:1–11. https://doi.org/10.1007/s11814-015-0065-3.
[42] Gao B, Jiang P, Lei H. Studies on adsorption property of novel composite adsorption material PEI/SiO2 for uric acid. Mater Lett 2006;60:3398–404.
[43] Jullok N, Van Hooghten R, Luis P, Volodin A, Van Haesendonck C, Vermant J, Van der Bruggen B. Effect of silica nanoparticles in mixed matrix membranes for pervaporation dehydration of acetic acid aqueous solution: plant-inspired dewatering systems. J Clean Prod 2016;112:4879–89.
[44] Kusworo TD, Al-Aziz H, Utomo DP. UV irradiation and PEG additive effects on PES hybrid membranes performance in rubber industry wastewater treatment. Proc. 2nd Int. Conf. Chem. Process Product Eng. 2020. https://doi.org/10.1063/1.5140921.
[45] Heikkinen JJ, Heiskanen JP, Hormi OEO. Grafting of functionalized silica particles with poly (acrylic acid). Polym Adv Technol 2006;17(6):426–9.
[46] Wu D, Huang Y, Yu S, Lawless D, Feng X. Thin film composite nanofiltration membranes assembled layer-by-layer via interfacial polymerization from polyethylenimine and trimesoyl chloride. J Membr Sci 2014;472:141–53.
[47] Al-Timimi DAH, Alsalhy QF, AbdulRazak AA, Drioli E. Novel polyether sulfone/polyethylenimine grafted nano-silica nanocomposite membranes: interaction mechanism and ultrafiltration performance. J Membr Sci 2022;659:120784.
[48] Al-Timimi DAH, Alsalhy QF, AbdulRaza AA. Polyethersulfone/amine grafted silica nanoparticles mixed matrix membrane: a comparative study for mebeverine hydrochloride wastewater treatment. Alex Eng J 2023;66:167–90.
[49] Figueroa RAR, Cassano A, Drioli E. Ultrafiltration of orange press liquor: optimization for permeate flux and fouling index by response surface methodology. Sep Purif Technol 2011;80:1–10.
[50] Noordina MY, Venkatesh VC, Sharif S, Elting S, Abdullah A. Application of response surface methodology in describing the performance of coated carbide tools when turning AISI 1045 steel. J Mater Process Technol 2004;145:46–58.

[51] Tanyildizi MS, Ozer D, Elibol M. Optimizationof a-amylase production by Bacillus sp. Using response surface methodology. Process Biochem 2005;40:2291–6.
[52] Bezerra MA, Santelli R, Oliveira EP, Villar LS, Escaleira LA. Response surface methodology (RSM) as a tool for optimization in analytical chemistry. Talanta 2008;76:965–77.
[53] Alsalhy QF, Albyati T, Zablouk M. A study ofthe effect of operating conditions on the reverse osmosis membrane performance with and without air sparging technique. Chem Eng Commun 2013;200:1–19.
[54] Rashid KT, Rahman SBA, Alsalhy QF. Optimum operating parameters for hollow fiber membranesin direct contact membrane distillation. Arabian J Sci Eng 2016;41:2647–58.
[55] Djebri A, Sadaoui Z, Belmedani M, Domergue L, Trari M. Removal efficiency of pharmaceutical drugs (Mebeverine hydrochloride MEB) by an activated carbon prepared from dates stems. J Environ. Health Sci. Engineer 2021:1–15. https://doi.org/10.1007/s40201-021-00658-1.
[56] Al-Khazrajy OSA, Boxall ABA. Risk-based prioritization of pharmaceuticals in the natural environment in Iraq. Environ Sci Pollut Res 2016:15712–26.
[57] Mohammad S, Reza R, Afshin M, Ali J, Mahdi S, Behzad S, Hiua D, Seung-Mok L. Synthesis and characterization of nanocomposite ultrafiltration membrane (PSF/PVP/SiO_2) and performance evaluation for the removal of amoxicillin from aqueous solutions. Environmental Technology & Innovation; 2019. p. 1–37. https://doi.org/10.1016/j.eti.2019.100529.
[58] Vatanpour V, Madaeni SS, Khataee AR, Salehi E, Zinadini S, Monfared HA. TiO2 embedded mixed matrix PES nanocomposite membranes: influence of different sizes and types of nanoparticles on antifouling and performance. Desalination 2012;292:19–29.
[59] Rasheed SH, Ibrahim SS, Alsalhy QF, Salih IK. Separation of soluble benzene from an aqueous solution by pervaporation using a commercial polydimethylsiloxane membrane. Membranes 2022;12:1040.
[60] Al-Dahri T, AbdulRazak AA, Khalaf IH, Rohani S. Response surface modeling of the removal of methyl orange dye from its aqueous solution using two types of zeolite synthesized from coal fly ash. Materials Express 2018;8(3):234–44.